Available online at www.sciencedirect.com

ScienceDirect

Procedia CIRP 111 (2022) 475–478

www.elsevier.com/locate/procedia

12th CIRP Conference on Photonic Technologies [LANE 2022], 4-8 September 2022, Fürth, Germany

The durability of stainless steel-polyamide laser joined assemblies

Mahdi Amne Elahi[a,*], Peter Plapper[a]

[a] University of Luxembourg, 6, rue Coudenhove-Kalergi, L-1359, Luxembourg

* Corresponding author. Tel.: +352-466644-5885; fax: +352-466-644-35885. E-mail address: mahdi.amneelahi@uni.lu

Abstract

Weight reduction and consequently less carbon footprint is one of the major goals in the automotive industry. This aim is addressed by laser joining of metals to polymers. However, the performance and long-time durability of the assemblies are the controversial aspects of this emerging technology. Therefore, the shear load and durability of the joints between stainless steel 304 and PA6.6 are addressed via different laser-based surface pretreatments on the metal. Microscopic evaluations are also implemented to examine the relationship between the surface condition of stainless steel and the performance of the assemblies. Considering the effect of pretreatments on the surface of the stainless steel, oxidizing the metal is favorable to improve the shear load of the joint assemblies, however, it is detrimental to the corrosion resistance due to the loss of alloying elements such as chromium and nickel.

Keywords: laser joining of SS/PA; laser-based surface treatment; tensile-shear test; durability

1. Introduction

Manufacturing of miniaturized, lightweight assemblies is one of the major goals in the automotive industry to reduce fuel consumption. In this regard, laser joining is the most versatile and predominant technology for several material combinations thanks to the unique properties of the laser beam [1,2]. Tailoring assemblies from different materials combinations enables us to take advantage of miscellaneous properties for a specific application in a single assembly. In this regard, stainless steel 304 and polyamide are some of the materials widely used in automotive industries, and manufacturing their assemblies with LAMP joining is interesting.

For several laser-joined metal/polymer assemblies the mechanism of bonding at the interface is reported. For instance, the metal-Cr-O-plastic for SS 304 joined to PET [3] or PA66 [4], Zn-O-C bond for ABS joined to Zn-coated steel [5]. In the case of aluminum laser-joined to PA, a correlation between the tensile-shear strength of the assembly and the thickness of the artificial aluminum oxide layer is reported [6]. In other studies, the formation of bonding at the interface of aluminum/PA via oxygen atoms of the aluminum oxide is introduced as the bonding mechanism [7-9]. Therefore, the presence of oxygen atoms in the metal's oxide is necessary to create a reliable bonding to the polymeric partner during the laser joining process. Several surface treatments are presented for aluminum and PA laser joined assemblies in order to modify the surface structure and chemistry of the joining components [9]. The enhancement of mechanical performance via enabling the mechanical interlocking for assemblies is also addressed [10].

Nomenclature

LAMP	Laser-Assisted Metal and Plastic
SS 304	Stainless Steel 304
PET	Polyethylene terephthalate
PA	Polyamide
ABS	Acrylonitrile Butadiene Styrene
SEM	Scanning Electron Microscopy
EDX	Energy Dispersive X-ray spectroscopy
CW/PW	Continuous/Pulsed Wave

10.1016/j.procir.2022.08.073

The effect of surface structuring and the laser joining parameters on the mechanical performance of the SS 304/PA assemblies produced by laser transmission joining is discussed [11]. Therefore, it is interesting to study the surface treatments of SS 304 with SEM-EDX and improve the adhesion via surface oxidation and address the performance of the assemblies with the combination of the mechanical and durability tests for the laser conduction joining process which is missing in the literature.

2. Experimental setup

The laser-based surface treatments are carried out on SS 304 samples in two categories of macro and micro treatments. The treated area is 30×10 mm for all samples. The macro treatment is implemented with a CW fiber laser (TruFiber 400 from Trumpf) equipped with Scanlab HS20 2D f-θ scanner. The process parameters were optimized to avoid warping the sample due to heat accumulation. The micro treatments are done in PW mode and by an Nd:YVO_4 laser (TruMark 6130 from Trumpf). The corresponding parameters for surface treatments are presented in Table 1.

Table 1. The parameters of laser-based surface treatments for SS 304.

	Type	CW laser Power [W]	Pulse frequency [kHz]	Scanning speed [mm/s]	Focal point
macro treatment	CW	400	-	7000	+8 mm from the surface
micro treatment	PW-1	4	120	750	On the surface
	PW-2	2.4	1	50	On the surface
	PW-3	16	40	300	On the surface

For the laser conduction joining process between SS 304 samples (60×30×0.5 mm) and conditioned PA6.6 (75×25×4 mm) according to ISO 1110, a disc laser (TruDisk 2000 from Trumpf) equipped with an intelliSCAN 30 FT optics (from Scanlab) controlled by an SCU-3 unit (from Blackbird) is used. SS 304 and PA are placed in an overlap configuration (overlap length is 12 mm) and the laser is applied from the SS side with a linear trajectory in the middle of the overlap. With the feed rate of 60 mm/s and the power of 300 W in CW mode, consequently, the joining area between SS 304 and PA is approximately 25×1.75 mm. The mechanical performance of the assemblies is evaluated by the tensile-shear test in a single lap configuration. The reported values are the average of at least three measurements. The durability of the samples is addressed by the salt spray test. The salt spray test is carried out with 5% Sodium Chloride at 35℃ for 500 hours.

3. Results

3.1. Different surface treatments

Table 2 depicts the average surface roughness (of at least five measurements) for SS 304 samples with different laser treatments. The Ra value of samples in untreated condition and treated with CW and PW-1are comparable and for sample PW-2, the increase is minor. However, sample PW-3 shows significantly more surface roughness.

Table 2. The Ra measurements for SS 304 surfaces with different treatments.

	untreated	CW	PW-1	PW-2	PW-3
Ra [µm]	0.1	0.09	0.12	0.17	2.87

Fig. 1(a) shows the SS 304 surface in an untreated condition. It is presented as the reference for further comparisons and Fig. 1(b) depicts the SS 304 surface in macro-treated condition (CW). A uniform sub-micron structure is observed on the surface due to very limited surface melting in thickness followed by a high cooling rate. Fig. 1(c) shows the micro-treated surface type PW-1. In this case, the surface of the metal is melted by a pulsed laser in a controlled manner that rounded the surface asperities. However, the extent of surface modification does not significantly impact surface roughness and these surfaces present approximately similar Ra values.

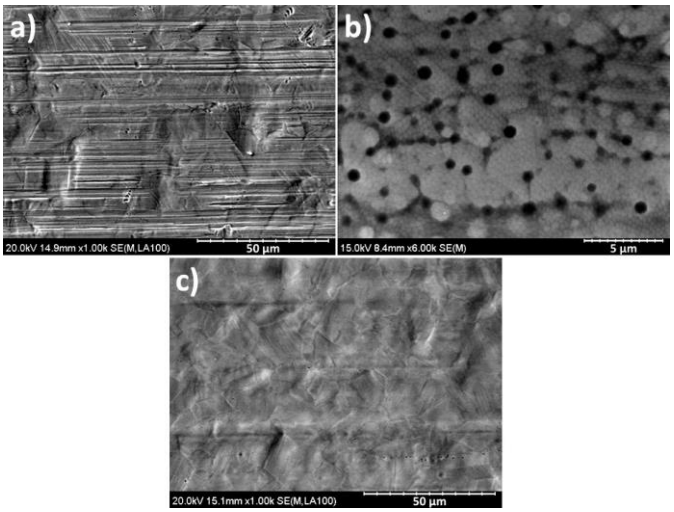

Fig. 1. Top-view SEM images of (a) untreated SS 304 sample, (b) after CW treatment, and (c) after PW-1 treatment.

Fig. 2 shows the PW-2 surface in two magnifications. The impact of individual pulses on the surface of SS 304 is visible due to lower pulse frequency (and consequently higher peak pulse power) compare to sample PW-1. The molten material is pushed to the surrounding of the laser spots which remains as a minor bulge upon solidification and slightly increases the surface roughness.

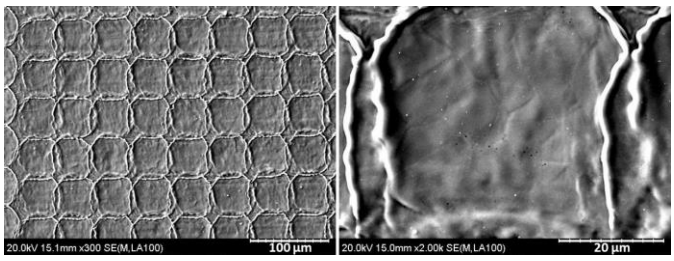

Fig. 2. Top-view SEM images of SS 304 surface after PW-2 treatment.

Fig. 3 depicts the PW-3 surface in two magnifications. The effect of implementing higher power compared to the previous PW samples is clear in the form of surface ablation of SS 304. The frozen droplets of molten materials trying to detach from the surface show the combination of surface melting and evaporation which consequently increases the surface roughness significantly compared to the previous samples.

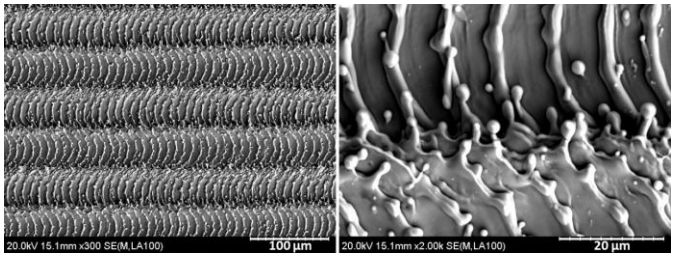

Fig. 3. Top-view SEM images of SS 304 surface after PW-3 treatment.

Fig. 4 presents the atomic percentage of alloying elements for different SS 304 samples carried out by EDX analysis. For untreated and treated samples with CW and PW-1 conditions, the chemical composition is more or less similar due to limited surface melting and only a slight surface cleaning effect is observed by reduction of carbon content. However, for PW-2 and PW-3 samples, the oxidation effect of the laser treatment process is observed. The loss of alloying elements and more specifically Cr and Ni is noticed for PW-2 and PW-3 samples.

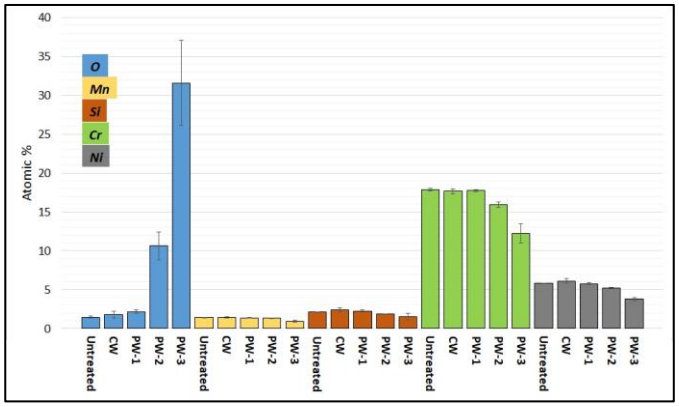

Fig. 4. The atomic percentage of alloying elements for samples with different surface treatments.

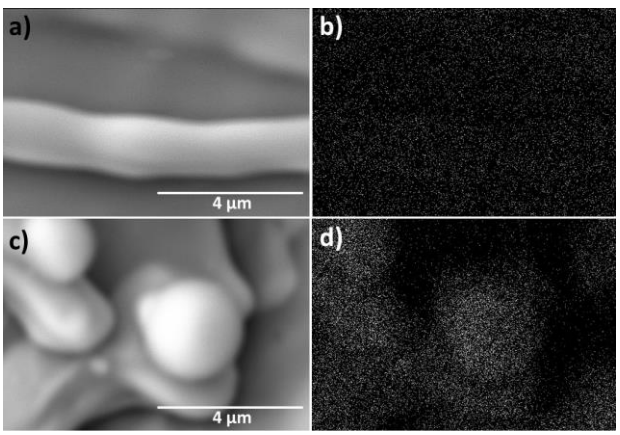

Fig. 5. a) SEM image of PW-1 surface, b) the corresponding oxygen elemental mapping for, c) SEM image of PW-3 sample, and d) the corresponding oxygen elemental mapping.

Fig. 5 depicts the elemental mapping of oxygen for samples PW-1 and PW-3. A significant oxidation effect due to extensive surface melting during the PW-3 process is observed compared to PW-1 and consequently other samples for this study. The concentration of oxygen atoms is visible on the molten droplets on the surface of the metal.

3.2. Mechanical performance of the assemblies

Fig. 6 depicts the mechanical performance of SS 304 samples with different surface conditions laser-joined to PA as described in section 2 (experimental setup). All laser treatment processes provide a higher tensile-shear load of the assembly compared to untreated condition. However, for this study, as the joining process is identical for all samples, a higher oxygen content of the SS 304 surface results in a higher tensile-shear load.

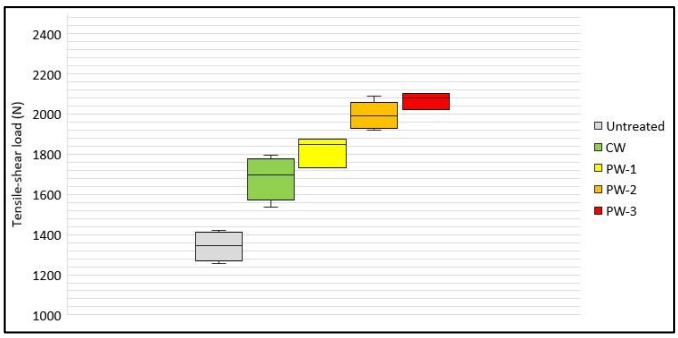

Fig. 6. Tensile-shear load of different SS 304 samples laser-joined to PA.

3.3. Salt-spray test

After 500 hours of the salt-spray test, the assemblies with PW-2 and PW-3 surface treatments of SS 304 present the highest mechanical performance with approximately 60% reduction in their maximum tensile-shear load. Other samples cannot maintain their mechanical performance after the test. Nevertheless, the corrosion behavior of SS 304 samples is opposite of the mentioned observation. Samples PW-2 and PW-3 suffer from the most significant corrosion after the test, while samples CW and PW-1 represent the highest corrosion resistance.

4. Discussions

Considering the laser treatments as non-contact processes, they provide a reliable cleaning effect for the samples. Consequently, regardless of further effects on the SS 304 surface, increasing the tensile-shear load of the assemblies with laser surface treatments is recorded compared to the untreated condition. The laser-treated samples can be classified into two categories: first the samples with similar surface roughness to the untreated state of SS 304 and slight oxidation effect during the treatment process, i.e., CW and PW-1 and then the samples with considerable surface oxide which follows by an increase in the surface roughness due to extensive surface melting, i.e., PW-2 and specifically PW-3.

The former category benefits from effective heat conduction from SS to PA surface thanks to the low surface roughness. Moreover, preserving the alloying elements (more specifically Cr and Ni) leads to the high corrosion resistance of this category during the salt-spray test. The formation of uniform, submicron grain structure on the surface of CW treated samples is also noticeable (see Fig. 1(b)) which results in high corrosion resistance. The shear loads of the samples for this category are in the medium range due to the presence of limited oxygen content on the surface, however, higher than that of untreated samples thanks to the cleaning effect of the laser treatment processes. The latter category, however, benefits from high oxygen contents on the surface which brings the high mechanical performance of the assemblies thanks to the increase of bonding regions. Regarding sample PW-2 the rise of surface roughness is not significant therefore, the majority of the contribution to the shear load originates from the oxygen content. Yet, the high surface roughness of sample PW-3 provides anchoring places for mechanical interlocking in addition to the chemical bonding to PA. At this stage, it is not feasible to quantify the contribution of the mechanical interlocking and chemical bonding separately. High surface roughness also boosts chemical bonding by providing more surface for bonding. In addition, increasing the surface roughness can be detrimental to the joint performance at the given laser joining process due to higher contact resistance between the materials which restricts the heat conduction from SS 304 to PA and consequently reduces the size of the joining area. Yet, it is not observed in the presented samples of this study. In conclusion, by comparing the mechanical performance of different samples for this study, it can be said that the decisive parameter to increase the shear load is the surface chemistry, i.e. oxygen content and surface cleaning effect of laser treatment, and the mechanical interlocking can improve the shear load up to a certain extend.

Nevertheless, the latter category is susceptible to corrosion due to the loss of Cr and Ni which provide good corrosion resistance for the metal. It is worth mentioning that the overlap between SS 304 and PA samples in the assembly is higher than the effective joined area. Therefore, the overlap area without contact between the materials acts as a place to stack up the corrosion products due to the capillary effect and deteriorates the mechanical performance over time by applying long-term peeling force on the joints. To sum up, the assemblies with higher oxygen contents at the surface of SS 304 show better long-term durability thanks to the stronger and more reliable joints between SS 304 and PA although they suffer from corrosion of 304 SS base material. To better examine the salt-spray test, the joining configuration needs to be modified regarding the overlap and laser-joining areas.

Conclusion

Based on the presented study regarding the laser-based surface treatments of SS 304 followed by their corresponding effect on the performance and durability of the laser-joined assembly with PA the followings are concluded:

- Improving the chemical bonding via surface oxidation and mechanical interlocking via increasing the surface roughness can improve the shear load of the assemblies. However, the contribution of chemical bonding is more significant.
- Increasing the oxygen content by applying a pulsed laser on the surface of SS 304 results in the loss of alloying elements such as Cr and Ni. Consequently, the corrosion resistance of SS 304 deteriorates.
- The formation of the uniform, sub-micron grain structure by the CW treatment of the SS 304 improves the corrosion resistance of the metal.
- The robustness of the bonding areas which is enhanced by a higher concentration of oxygen atoms can provide long-term durability for the assembly. However, some design aspects regarding the width of the overlap and the joining area are also influential.

Acknowledgements

The presented work is based on ‘‘Process Innovation for Sensors in Mobile Applications Based on Laser Assisted Metal-Plastic Joining’’ project (AFR-PPP grant, Reference 11633333). The authors would like to thank the financial support of the Luxembourg National Research Fund (FNR) and appreciate Cebi Luxembourg S.A. as the industrial partner of the project.

References

[1] Amne Elahi M, Plapper P. Dissimilar laser micro-welding of nickel wire to CuSn6 bronze terminal. Trans. Indian Inst. Met. 2019;72: 27-34.
[2] Schricker K, Bergmann JP. Determination of sensitivity and thermal efficiency in laser assisted metal-plastic joining by numerical simulation. Procedia CIRP 2018;74:511-517.
[3] Katayama S, Kawahito Y. Direct joining of metal and plastic with laser. Scr. Mater. 2008;59:1247-1250.
[4] Gao M, Liao W, Chen C. Improving the interfacial bonding strength of dissimilar PA66 plastic and 304 stainless steel by oscillating laser beam. Opt. Laser Technol. 2021;138(106869).
[5] Jung DJ, Cheon J, Na SJ. Effect of surface pre-oxidation on laser assisted joining of acrylonitrile butadiene styrene (ABS) and zinc-coated steel. Mater. Des. 2016;99:1-9.
[6] Heckert A, Singer C, Zaeh MF. Pulsed laser surface pre-treatment of aluminium to join aluminium- thermoplastic hybrid parts. Lasers in Manufacturing (LiM) conference, Germany, 2015.
[7] Bartha JW, Hahn PO, LeGoues F, Ho PS. Photoemission spectroscopy study of aluminum–polyimide interface. J. Vac. Sci. Technol. A: Vacuum, Surfaces, and Films 1985;3:1390-1393.
[8] Hirchenhahn P. Fundamental study of the adhesion phenomena in polymer-metal hybrid materials obtained by laser welding, Ph.D. thesis, University of Namur, Belgium, 2020.
[9] Amne Elahi M, Koch M, Plapper P. Evaluation of the joint based on different surface conditions for aluminum-polyamide laser welding. J. Laser Appl. 2021;33(012036).
[10] Roesner A, Scheik S, Olowinsky A, Gillner A, Reisgen U, Schleser M. Laser assisted joining of plastic metal hybrids. Physics Procedia 2011;12:370-377.
[11] Cenigaonaindia A, Liébana F, Lamikiz A, Echegoyen Z. Novel strategies for laser joining of polyamide and AISI 304. Physics Procedia 2012;39:92-99.